Supplementary Information

CoFe nanoalloys encapsulated in nitrogen-doped carbon for efficient nitrite electroreduction to ammonia

Dongdong Zhu, [a] Binbin Zhang, [b] Junlong Chen, [b] Fangxi Xie, [c] Yan Zou [a] and Ping Chen * [b]

[a] School of Chemistry and Materials Science, Institute of Advanced Materials and Flexible Electronics (IAMFE), Nanjing University of Information Science and Technology, Nanjing, 210044, China

[b] School of Materials Science and Engineering, Anhui University, Hefei, Anhui, 230601, China E-mail: chenping@ahu.edu.cn

[c] Department of Chemical Engineering, The University of Melbourne, Victoria, 3010, Australia

1. Experimental Section

1.1 Catalyst Synthesis

CoFe-PBA was synthesized by a typical co-precipitation method. In detail, 120 mL aqueous solution with 1.6 mmol $K_3[Fe(CN)_6]$ was slowly added into 80 mL aqueous solution containing 2.4 mmol $Co(NO_3)_2 \cdot 6H_2O$ and 2.0 mmol $Na_3C_6H_5O_7 \cdot 2H_2O$ under stirring. The obtained solution was stirred for another 30 min and then aged in a round flask at 80 °C for 6.0 h. Finally, the precipitate was collected via centrifugation, washed with water and ethanol for several times, and dried by vacuum freeze-drying overnight. CoFe-NC sample was fabricated via annealing CoFe-PBA precursor under N_2 protection. The obtained CoFe-PBA powder was put into a tube furnace and calcined in N_2 atmosphere at 600 °C for 2.0 h, and the heating rate is 5 °C min^{-1}. For comparison, CoFe-NC-500, and CoFe-NC-700 samples were prepared via annealing CoFe-PBA precursor under N_2 protection at 500 ℃, and 700 ℃, respectively. Moreover, CoFe-PBA was annealed at 600 ℃ for 2 hours in air to synthesize CoFe oxide, then the as-fabricated CoFe oxide was annealed at 650 ℃ for 1 hour in 5% H_2/Ar to fabricate CoFe alloy sample.

1.2 Material characterization

The morphology of the products was characterized by a scanning electron microscope (SEM, HITACHI Regulus 8230, Japan), and a field emission transmission electron microscope (JEOL JEM 2100, Japan). The crystal phase of the products was characterized by a powder X-ray diffraction (XRD, Rigaku SmartLab 9KW with Cu-kα radiation, λ=0.15406 nm) from 10 to 90° with a rate of 10° min^{-1}. XPS data of the

products were obtained using a Thermo ESCALAB 250Xi X-ray photoelectron spectrometer (Thermo ESCALAB 250Xi, USA). The X-ray absorption spectrum (XAS) was conducted on TableXAFS-500 (Specreation Instruments Co., Ltd., China). The iron and cobalt contents were determined using an inductively coupled plasma mass spectrometer (ICP-MS, Thermo Scientific).

1.3 Electrochemical measurement

All electrochemical measurements were carried out in a H-type electrolytic cell separated by a treated Nafion 117 membrane (DuPont, USA) using the CHI 750E electrochemical workstation (Shanghai, Chenhua) under the ambient conditions. The CoFe-NC powder coated on carbon paper (1.0×1.0 cm^2), Ag/AgCl electrode, and platinum foil were used as the working electrode, reference electrode and counter electrode, respectively. The electrolyte used was 0.1 M phosphate buffer solution (PBS) with 0.1 M $NaNO_2$. All the potentials were converted to the reversible hydrogen electrode (RHE). In this work, only LSV curves were 90%*IR corrected. The chronoamperometry test was performed at different potentials for 1.0 h.

1.4 Determination of NH_3

Concentration of produced NH_3 was quantitatively determined by the indophenol blue method. In brief, 5.0 g of sodium salicylate, 5.0 g of trisodium citrate dihydrate, and 4.0 g of NaOH were dissolved in 100.0 mL deionized water (Reagent A). Reagent B is configured with 0.05 M NaClO. 0.5 g of sodium nitroferricyanide was dissolved in 50.0 mL deionized water (Reagent C). 6.0 mL of the diluted catholyte was obtained

from the cathodic chamber and mixed with 6.0 mL of Reagent A, 3.0 mL of Reagent B and 0.6 mL of Reagent C. After standing for 2 h at room temperature, the ultraviolet-visible absorbance was measured at 660 nm on UV-Vis spectrophotometer (UV-1800, Shimadzu, Japan). The concentration-absorbance calibration curve was obtained using standard NH_4Cl solution with varying concentration.

1.5 Calculations of FE and yield of NH_3

$FE = (6 \times F \times [NH_3] \times V) / (M_{NH3} \times Q) \times 100\%$

NH_3 yield $= ([NH_3] \times V) / (M_{NH3} \times t \times S)$

Where F is the Faradic constant (96485 C mol^{-1}), $[NH_3]$ is the measured NH_3 concentration, V is the volume of electrolyte in the anode compartment, M_{NH3} is the molar mass of NH_3, Q is the total quantity of applied electricity, t is the electrolysis time, S is the loaded area of catalyst.

2. Supplementary Figures and Tables

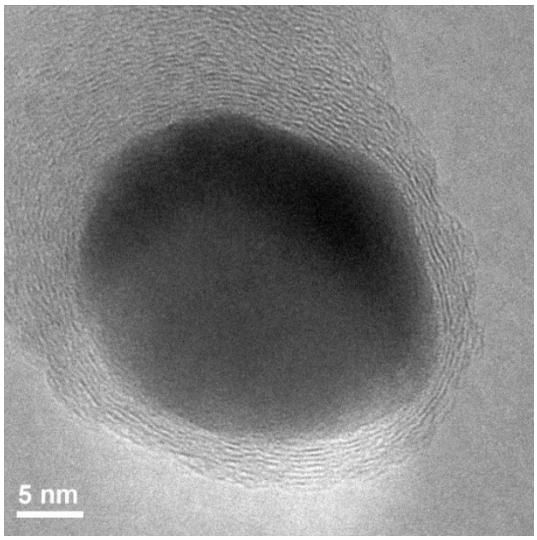

Figure S1. HRTEM image of CoFe-NC.

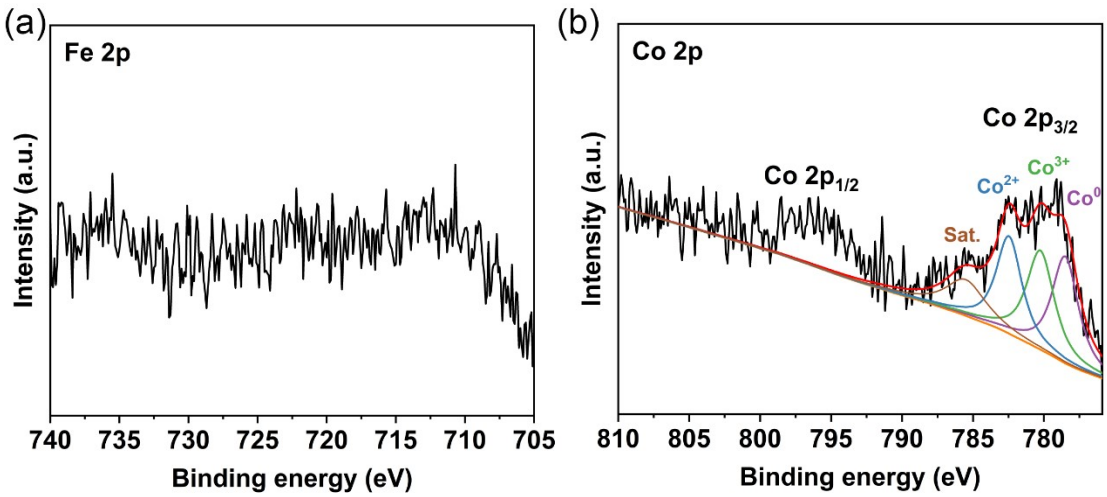

Figure S2. XPS spectra of (a) Fe 2p and (b) Co 2p for CoFe-NC.

The XPS signal of Fe 2p and Co 2p is relatively weak, which can be attributed to the fact that XPS is a surface-sensitive technique, while CoFe alloy is coated by nitrogen-doped carbon in CoFe-NC. Such phenomenon was also reported by previous work (J. Mater. Chem. A, 2022, 10, 8378). Notably, the Co^0 species in figure S2b also verifies the existence of metallic CoFe alloy in CoFe-NC. Moreover, the generation of high-valence metal peaks could be attributed to the formation of N-metal bonds (J. Energy Chem. 2021, 61, 327; Appl. Catal. B 2021, 298, 120512).

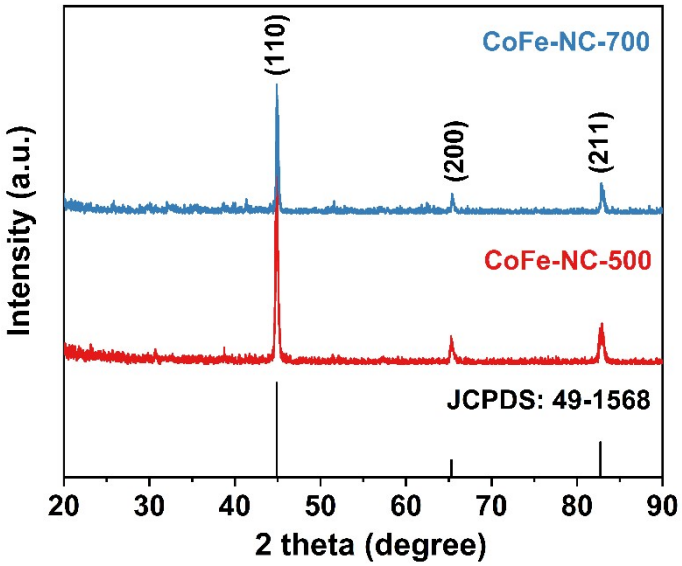

Figure S3. XRD patterns of CoFe-NC-500, and CoFe-NC-700 samples.

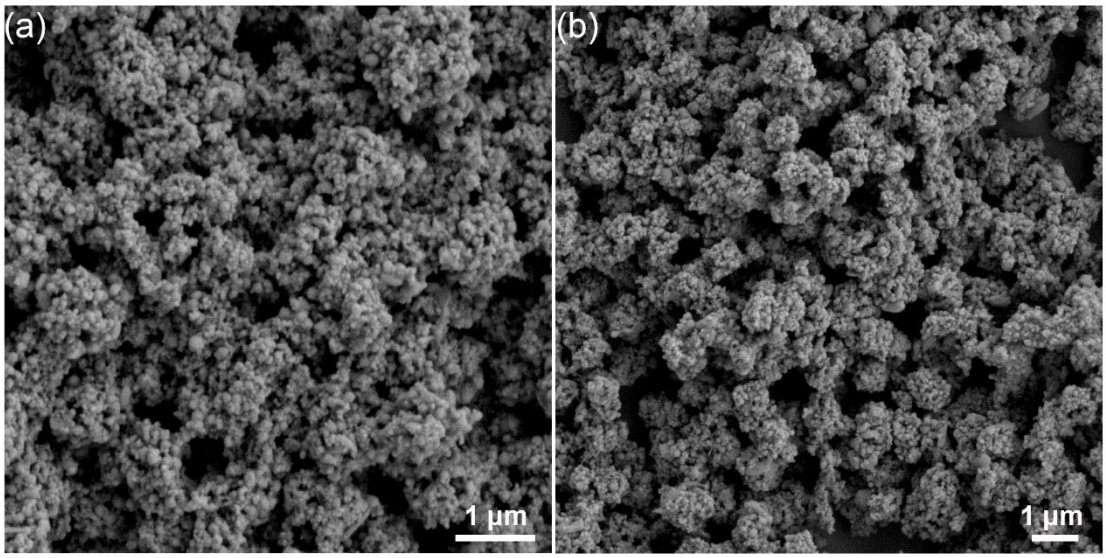

Figure S4. (a) SEM image of CoFe-NC-500 sample, (b) SEM image of CoFe-NC-700 sample.

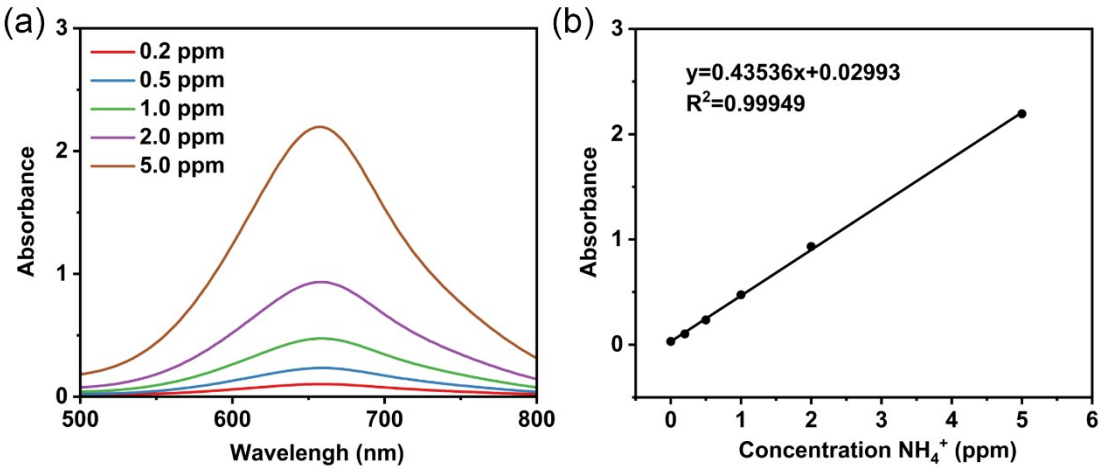

Figure S5. (a) UV-Vis absorption curves of indophenol assays kept with different concentrations of NH^{4+} ions for 2 h at room temperature. (b) Calibration curve used to estimate the concentration of NH^{4+} concentration.

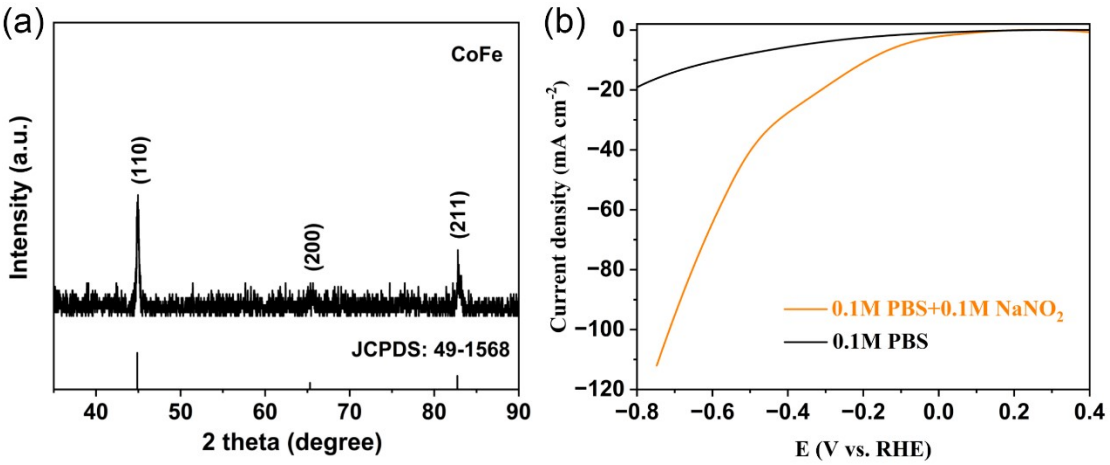

Figure S6. (a) XRD pattern of CoFe alloy sample. (b) LSV curves of CoFe alloy in 0.1 M PBS with/without 0.1 M $NaNO_2$.

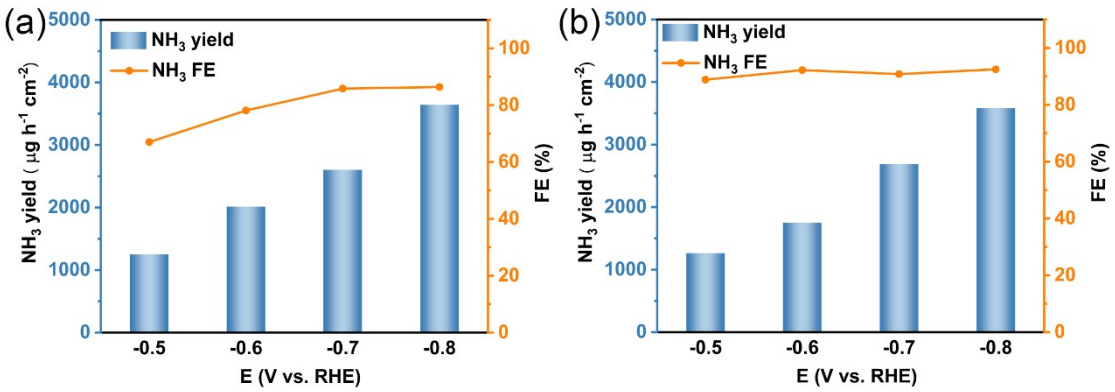

Figure S7. (a) NH_3 yields and FEs of CoFe-NC at different applied potentials in 0.25 M PBS with 0.1 M $NaNO_2$. (b) NH_3 yields and FEs of CoFe-NC at different applied potentials in 0.1 M SO_4^{2-} with 0.1 M $NaNO_2$.

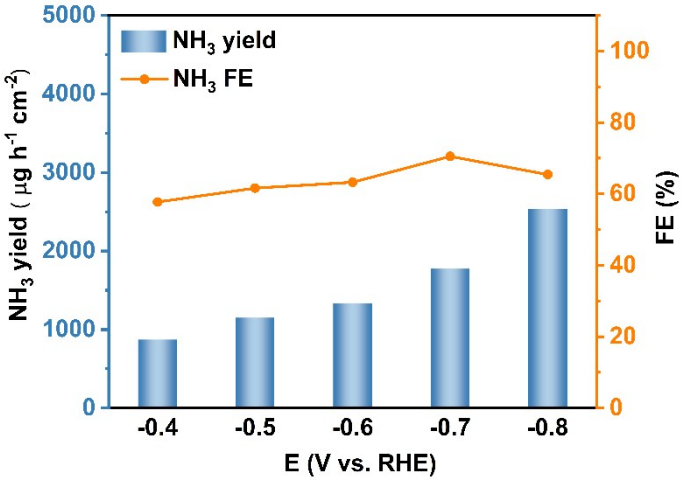

Figure S8. NH_3 yields and FEs of CoFe-NC-500 at different applied potentials in 0.1 M PBS with 0.1 M $NaNO_2$.

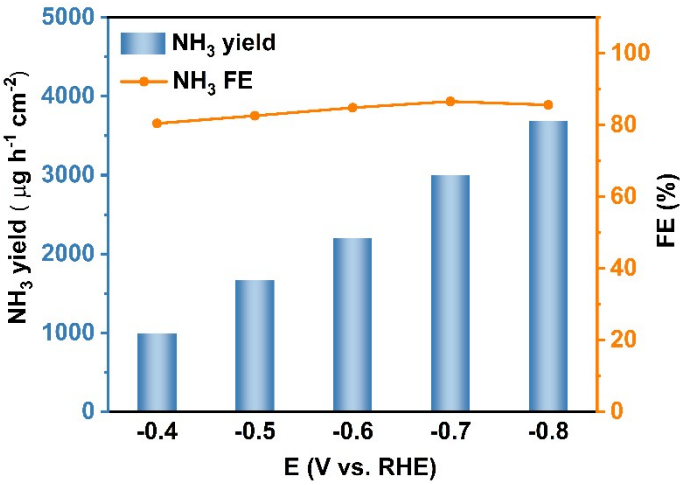

Figure S9. NH_3 yields and FEs of CoFe-NC-700 at different applied potentials in 0.1 M PBS with 0.1 M $NaNO_2$.

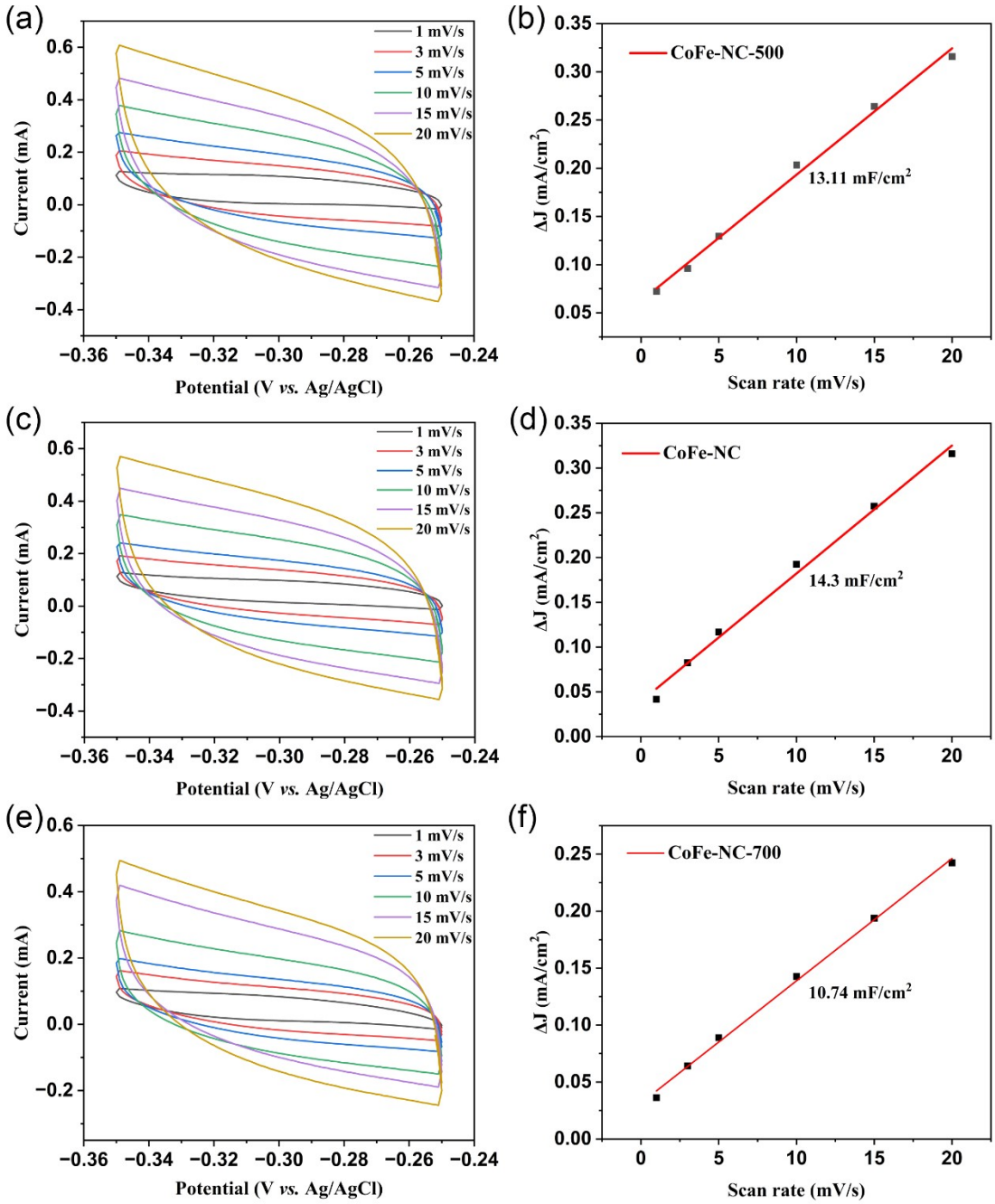

Figure S10. Cyclic voltammograms (CV) curves for (a) CoFe-NC-500, (c) CoFe-NC, and (e) CoFe-NC-700 samples at the scan rates from 1 to 20 mV/s. Current density as a function of the scan rate to give the double-layer capacitance (C_{dl}) of (b) CoFe-NC-500, (d) CoFe-NC, and (f) CoFe-NC-700.

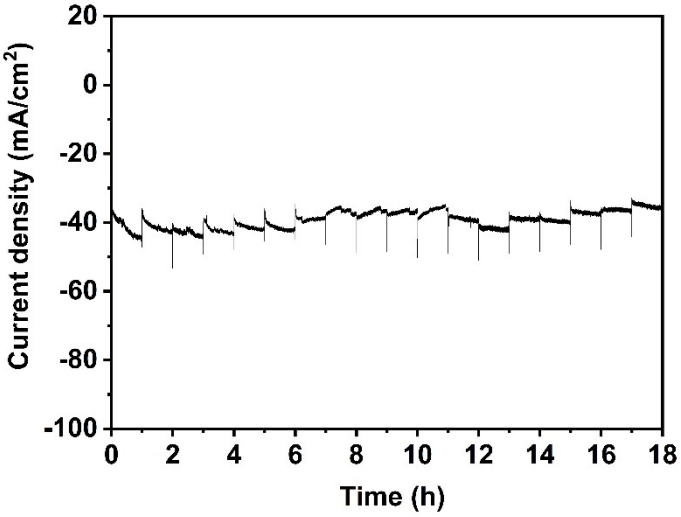

Figure S11. Chronoamperometry curve of CoFe-NC performed at –0.65 V vs. RHE (without IR correction) in 0.1 M PBS with 0.1 M $NaNO_2$.

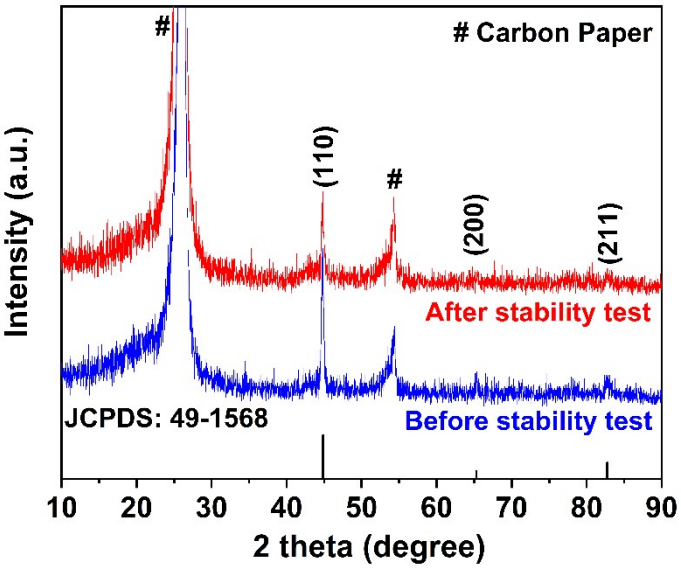

Figure S12. XRD patterns of CoFe-NC sample coated on carbon paper before and after stability test.

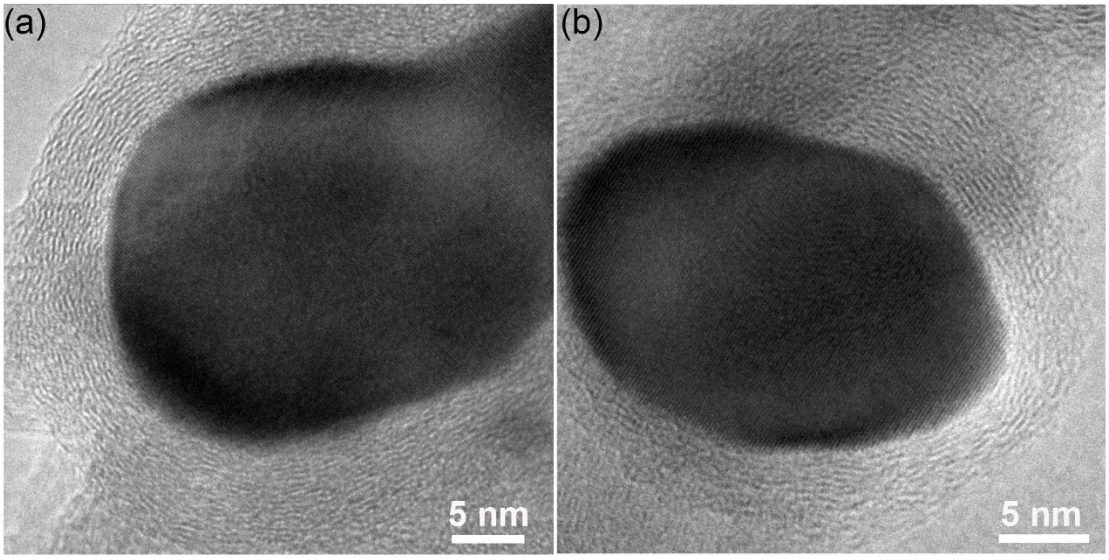

Figure S13. TEM images of CoFe-NC sample after stability test.

Table S1. Atomic percentage of corresponding elements in CoFe-NC by XPS analysis.

	C 1s	N 1s	O 1s	Fe 2p	Co 2p
Atomic %	64.55	11.13	22.67	0.83	0.82

Table S2. Summary of the performance of recently reported nitrite reduction reaction

electrocatalysts.

Catalyst	Electrolyte	Potential	Performance	Ref.
CoFe-NC	0.1 M PBS with 0.1 M NO_2^-	−0.7 V (*vs.* RHE)	FE (NH_3) = 94.5% NH_3 yield = 3.44 mg h^{-1} cm^{-2}	This work
CoP	0.1 M PBS with 500 ppm NO_2^-	−0.2 V (*vs.* RHE)	FE (NH_3) = 90% NH_3 yield = 2.26 mg h^{-1} cm^{-2}	1
Cu_3P	0.1 M PBS with 0.1 M NO_2^-	−0.5 V (*vs.* RHE)	FE (NH_3) = 91.2% NH_3 yield = 1.62 mg h^{-1} cm^{-2}	2
FeP	0.05 M Na_2SO_4 with 80 mg L^{-1} NO_2^-	−0.5 V (*vs.* RHE)	FE (NH_3) = 82.5%	3
Ni-NSA-V_{Ni}	0.2 M Na_2SO_4 with 200 ppm NO_2^-	−1.2 V (*vs.* SCE)	FE (NH_3) =88.9% NH_3 yield = 0.23 mmol h^{-1} cm^{-2}	4
Pd/CuO	0.1 M K_2SO_4 with 0.01 M NO_2^-	−1.5 V (*vs.* SCE)	FE (NH_3) =91.8% NH_3 yield = 0.906 mg h^{-1} mg_{cat}^{-1}	5
Cobaloximes/ MWCNT	0.1 M PBS with 0.1 M NO_2^-	−0.5 V (*vs.* RHE)	FE (NH_3) = 95% NH_3 yield = 19.3 mg h^{-1} mg_{cat}^{-1}	6
Ni@MDC	0.1 M NaOH with 0.1 M NO_2^-	−0.8 V (*vs.* RHE)	FE (NH_3) = 65.4% NH_3 yield = 6.3 mg h^{-1} mg_{cat}^{-1}	7
ITO@TiO_2	0.5 M $LiClO_4$ with 0.1 M NO_2^-	−0.5 V (*vs.* RHE)	FE (NH_3) = 82.6% NH_3 yield =0.41 mmol h^{-1} cm^{-2}	8
Ru SA-NC	1.0 M KOH with 0.5 M NO_2^-	−0.4 V (*vs.* RHE)	FE (NH_3) =97.8% NH_3 yield = 0.69 mmol h^{-1} cm^{-2}	9
Ag nanoarray	0.1 M NaOH with 0.1 M NO_2^-	−0.7 V (*vs.* RHE)	FE (NH_3) =90% NH_3 yield = 5.7 mg h^{-1} cm^{-2}	10
CoO_x	0.1 M KOH with NO_2^-	−0.3 V (*vs.* RHE)	FE (NH_3) = 94.4% NH_3 yield = 116.1 mg h^{-1} mg_{cat}^{-1}	11
Cu_2Pd	0.5 M KOH with 2.8 mg mL^{-1} NO_2^-	−0.2 V (*vs.* RHE)	FE (NH_3) = 90% NH_3 yield = 1.76 mg h^{-1} mg_{cat}^{-1}	12

References

1. G. Wen, J. Liang, Q. Liu, T. Li, X. An, F. Zhang, A. A. Alshehri, K. A. Alzahrani, Y. Luo, Q. Kong and X. Sun, *Nano Res.*, 2022, **15**, 972-977.
2. J. Liang, B. Deng, Q. Liu, G. Wen, Q. Liu, T. Li, Y. Luo, A. A. Alshehri, K. A. Alzahrani, D. Ma and X. Sun, *Green Chem.*, 2021, **23**, 5487-5493.
3. J. Yuan, H. Yin, X. Jin, D. Zhao, Y. Liu, A. Du, X. Liu and A. P. O'Mullane, *Appl. Catal. B*, 2023, **325**, 122353.
4. C. Wang, W. Zhou, Z. Sun, Y. Wang, B. Zhang and Y. Yu, *J. Mater. Chem. A*, 2021, **9**, 239-243.
5. S. Liu, L. Cui, S. Yin, H. Ren, Z. Wang, Y. Xu, X. Li, L. Wang and H. Wang, *Appl. Catal. B*, 2022, **319**, 121876.
6. S.-L. Meng, C. Zhang, C. Ye, J.-H. Li, S. Zhou, L. Zhu, X.-B. Li, C.-H. Tung and L.-Z. Wu, *Energy Environ. Sci.*, 2023, **16**, 1590-1596.
7. X. He, X. Li, X. Fan, J. Li, D. Zhao, L. Zhang, S. Sun, Y. Luo, D. Zheng, L. Xie, A. M. Asiri, Q. Liu and X. Sun, *ACS Appl. Nano Mater.*, 2022, **5**, 14246-14250.
8. S. Li, J. Liang, P. Wei, Q. Liu, L. Xie, Y. Luo and X. Sun, *eScience*, 2022, **2**, 382-388.
9. Z. Ke, D. He, X. Yan, W. Hu, N. Williams, H. Kang, X. Pan, J. Huang, J. Gu and X. Xiao, *ACS Nano*, 2023, **17**, 3483-3491.
10. Q. Liu, G. Wen, D. Zhao, L. Xie, S. Sun, L. Zhang, Y. Luo, A. Ali Alshehri, M. S. Hamdy, Q. Kong and X. Sun, *J. Colloid Interface Sci.*, 2022, **623**, 513-519.
11. J. Wang, C. Cai, Y. Wang, X. Yang, D. Wu, Y. Zhu, M. Li, M. Gu and M. Shao, *ACS Catal.*, 2021, **11**, 15135-15140.
12. W. Li, S. Zhang, J. Ding, J. Liu, Z. Wang, H. Zhang, J. Ding, L. Chen and C. Liang, *ACS Sustainable Chem. Eng.*, 2023, **11**, 1168-1177.